Plasma activation of N_2, CH_4 and CO_2: an assessment of the vibrational non-equilibrium time window

A.W. van de Steeg, T. Butterworth, D.C.M. van den Bekerom, A.F. Sovelas da Silva, M.C.M. van de Sanden, G.J. van Rooij

Dutch Institute for Fundamental Energy Research, 5612 AJ Eindhoven, The Netherlands

Abstract

Vibrational excitation potentially enhances the energy efficiency of plasma dissociation of stable molecules and may open new routes for energy storage and process electrification. Electron, vibrational and rotational temperatures were measured by in-situ Thomson and Raman scattering in order to assess the opportunities and limitations of the essential vibration-translation non-equilibria in N_2, CO_2 and CH_4 plasma. Electron temperatures of 1.1-2.8 eV were measured in N_2 and CH_4. These are used to confirm predominant energy transfer to vibrations after an initial phase of significant electronic excitation and ionization. The vibrational temperatures initially exceed rotational temperatures by almost 8000 K in N_2, by 900 K in CO_2, and by 300 K in CH_4. Equilibration is observed at the 0.1 ms timescale. Based on the vibrational temperatures, the vibrational loss rates for different channels are estimated. In N_2, vibrational quenching via N atoms is identified as the dominant equilibration mechanism. Atomic nitrogen population reaches a mole fraction of more than 1%, as inferred from the afterglow emission decay, and explains a gas heating rate of 25 $K\mu s^{-1}$. CH_4 equilibration at 1200 K is predominantly caused by vibrational-translational relaxation in CH_4-CH_4 collisions. As for CO_2, vibrational-translational relaxation via parent molecules is responsible for a large fraction of the observed heating, whereas product-mediated VT relaxation is not significantly contributing. It is suggested that electronic excitation, followed by dissociation or quenching contributes to the remaining heat generation. In conclusion, the time window to profit from vibrational excitation under the present conditions is limiting practical application.

Broader context

Efficient dissociation mechanisms of thermodynamically stable molecules will fulfill a pivotal role in the energy and industrial landscape of the future. As carbon cycles are to be closed and nitrogen fixation to become fossil fuel independent, efficient activation of CO_2, CH_4 and N_2 as chemical building blocks becomes essential. In this context, plasma technology is gaining attention as an alternative to conventional methods due to its compatibility with renewable energy intermittency and scalability. Moreover, it is widely theorized that preferential heating of molecular vibrations offers opportunities for breakthroughs in yield and efficiency. This paper provides a benchmark for

these speculations by a detailed characterization of vibrational heating specificity and timescales of quenching on basis of microscopic measurements and rate estimations for the splitting of CO_2, CH_4 and N_2.

Introduction

Molecular vibrations can significantly enhance energy efficiencies in the dissociation of thermodynamically stable molecules [1] in both the gas phase and coupled with catalysts [2]. In the gas phase, the efficiency of electron impact dissociation may be enhanced through more favorable Franck-Condon overlap between lower vibrational levels of ground state and products [3]. The high efficiency of vibration-driven chemistry is mainly attributed however to the vibrational ladder climbing process, analogous to vibrational pooling [4][5]. Here, stepwise vibrational excitation allows to break molecular bonds at the bond enthalpy [6][7]. This mechanism is the prevailing model for explaining the over 80% energy efficiency that was reported for the splitting of CO_2, where the vibrational excitation was provided by plasma electrons [8][9]. The anharmonicity of the molecule creates a preference in vibration-vibration (VV) collisions to up-excite molecules in higher vibrational levels compared to those in lower levels, thereby overpopulating the higher vibrational levels [10][11]. Low gas temperatures must be maintained under strong vibrational excitation conditions for ladder climbing to be effective [12]. Coupled with a catalyst, vibrational excitation is believed to provide an energetically favorable pathway in for example ammonia synthesis [2] or in providing selectivity to the non-oxidative coupling of methane [13]. Successful implementation of these schemes, similar to ladder climbing in the pure gas phase, requires abundant vibrational excitation preferably at low gas temperatures. Additionally, the lifetime of the vibrationally excited species must be of sufficient length to ensure interaction with the catalytic surface.

Plasma can be a suitable medium to achieve the required selective vibrational excitation. Under steady state conditions of moderate power density, vibrational excitation can be the primary energy transfer channel between the plasma electrons and the heavy particles [12]. The selectivity of the plasma in transferring electrical power to vibrations depends mainly on the electron temperature [14]. If the electron temperature gets above 2-3 eV, as often is the case in transient behavior, the electrons will deposit significant amounts of energy in electronic excitation [1]. The electronic states can cause dissociation, radiate or be quenched, which will cause gas kinetic heating or radiative heat losses and thus reduce efficiency [15].

To maintain a high vibrational non-equilibrium, the gas temperature must be kept low to suppress quenching of vibrations. Quenching of vibrational quanta to translational heat (VT relaxation) poses an inherent loss mechanism of vibrational energy, and limits the timescales in which the vibrational

chemistry can occur [11]. VT relaxation not only decreases the vibrational excitation density, but also increases the gas temperature. Because the rate of VT relaxation increases strongly with gas temperature [16], the gas temperature has to be kept as low as possible to prevent the undesired positive feedback loop between gas heating and quenching [15].

The present study compares three molecules: N_2, CO_2 and CH_4. Starting from a symmetric diatomic molecule and stepping up in atom number increases both the complexity and state density of the vibrational manifold as well as the chemistry. Nitrogen has a single mode of vibration for which ladder climbing has been demonstrated to lead to overpopulation of the higher levels. This yields a non-Boltzmann distributed vibrational distribution function (VDF) [17][18], such as a Treanor distribution [5]. CO_2 has four normal modes of vibrations (of which one doubly degenerate), where the high energy asymmetric stretch mode is decoupled from the low-energy bending and symmetric stretching modes (the latter two being coupled by Fermi resonance). CH_4 has 9 vibrational normal modes, a complexity for which such decoupling is no longer evident. Furthermore, the relaxation times of vibrations in CO_2 and CH_4 are respectively 3 and 4 orders of magnitude faster than for N_2 at similar conditions due to their resonances and low-energy vibrational constants [19][20]. This emphasizes the challenge of vibrationally driving chemistry in more complex molecules.

In addition to their scientific relevance, all three molecules also have societal impact in the context of the energy transition and climate change. Efficient dissociation of nitrogen for fertilizer production can potentially lower the large carbon footprint associated with the current Haber-Bosch production standard [21]. Efficient CO_2 dissociation into CO and O_2 will create opportunities for closing the carbon cycle. For example, it constitutes an alternative form of storing energy, i.e. in chemical bonds instead of in batteries, enabling large scale energy storage and transportation as well as sector integration [1][7]. Non-oxidative coupling of methane may open high efficiency pathways to value-added chemicals such as ethylene [22]. Here the methane molecules are first dissociated into CH_x radicals, which form larger carbon chains upon recombination [23].

For CO_2 plasma, extensive research has been reported in recent years on dissociation and vibrational kinetics in, both in low-power glow discharges [24][25][26] and in high power microwave discharges [27][28][29][30]. However, it remains unproven whether the mechanism of vibrational ladder climbing is the main dissociation pathway while none of the investigations reproduced the >80% energy efficiencies reported by Butylkin *et al.* [8] so far.

For nitrogen plasma, vibrational temperatures up to 10^4 K at gas temperatures less than 10^3 K have been reported in literature under specific conditions [17][31]. The large degree of non-equilibrium which can be obtained in N_2 is attributed to its slow quenching of vibrations, as previously

3

mentioned due to the large vibrational constant compared to typical translational energies [32]. However, atomic N, which is inherently produced in a plasma discharge, is an efficient quencher of vibrations, especially at higher temperatures and for high vibrational levels [17]. Nonetheless non-equilibrium conditions have also been observed in the periphery of continuous intermediate pressure N_2 plasmas, which do have a thermal core [33].

CH_4 plasma is traditionally receiving interest in view of non-oxidative coupling as an alternative to oxidative CH_4 reforming. However, it is limited by coke formation and selectivity problems [22][34][35]. In high-power microwave plasma, specific conditions with temperatures ranging from 1000 K to 2000 K were found without coke formation [36]. Nevertheless, selectivity and low energy efficiency remain as issues.

Vibrational energy transfer in these molecules has been studied extensively. For N_2 and CO_2, this was mainly in the context of the CO_2 laser [16][37][38][39]. The CO_2 laser operates on population inversion between the first excited asymmetric stretch vibrational level and the first Fermi resonant levels. Ladder climbing beyond the first level, the motivation within the present context, is specifically suppressed in the CO_2 laser by the addition of H_2 or H_2O [40]. CH_4 was a molecule of choice to study fundamental molecular energy transfer mechanisms. It was found that sustaining a non-equilibrium between the vibrational modes is more challenging because of the strong coupling of the four modes of vibration [20][41][42].

The present paper uses low duty-cycle pulsed plasma to assess the potential for achieving non-equilibrium in high-power microwave plasma. Pulsed operation is chosen over continuous plasma, as the latter is seen to have a high temperature thermal core for the considered molecules [33][36][43], thereby likely eliminating possible non-equilibrium benefits and creating conditions in which thermal chemistry dominates [27]. In the low duty cycle pulsing scheme adopted from Van den Bekerom [44], the plasma ignites at room temperature, which ensures minimal VT relaxation. Van den Bekerom estimated the reduced electric field based on an energy partition to the different degrees of freedom. This demonstrated a limited selectivity to vibrational modes, attributed to the low duty cycle and high electron losses. All experiments were performed with pure N_2, CH_4 and CO_2. Admixing noble gases [45] or alkali metals [28] may be attractive options for altering electron properties and is envisaged for future work.

The ultra-low duty cycle, high flow conditions ensure the gas is refreshed between pulses, eliminating product-induced effects on VT relaxation or electron properties at ignition. These plasmas are coupled with laser scattering to yield time resolved measurements of the energy fluxes to the different degrees of freedom. Thomson scattering and rotational and vibrational Raman

4

scattering respectively yield electron temperatures, rotational temperatures (which serve as a proxy for the gas temperature) and vibrational temperatures. Electron temperatures could only be resolved in N_2 and CH_4 plasma, where the absence of rotational Raman signature in CH_4 readily yields Thomson signal. In N_2 the well resolved Raman signal could be separated to yield a Thomson signature. Vibrational Raman scattering in N_2, analyzed following the analytical treatment of Long [46], gives rotational and vibrational temperatures. Vibrational Raman spectra of the CO_2 dyad are analyzed following the procedure described in our earlier work [44] to yield temperatures of the different vibrational modes, T_{12} and T_3, respectively belonging to the coupled symmetric/bending mode and the asymmetric stretch mode. Vibrational Raman in the pentad region of CH_4 yields both vibrational and rotational temperatures, as detailed in recent work of Butterworth et al. [47].

These time-resolved measurements allow us to unravel the importance of different heat transfer processes that may limit the time window of non-equilibrium in microwaves plasma. The aim is to establish how, and on what timescale gas heating and thermal equilibration will occur, and thus how long it is possible to sustain non-equilibrium under high-power conditions.

Method & Setup

The experimental layout is schematically shown in Figure 1. A solid state MW power source (Ampleon) applies 200 μs, 800 W peak power MW pulses via a WR340 waveguide to a 27 mm inner diameter quartz tube, where the plasma is generated. A three-stub tuner and an adjustable short are used to tune the electrical field to optimal conditions for electrical breakdown. Tangential gas injection leads to a swirl flow in the tube, which stabilizes the plasma. The flow and pressure are fixed at 4 slm and 25 mbar for all experiments.
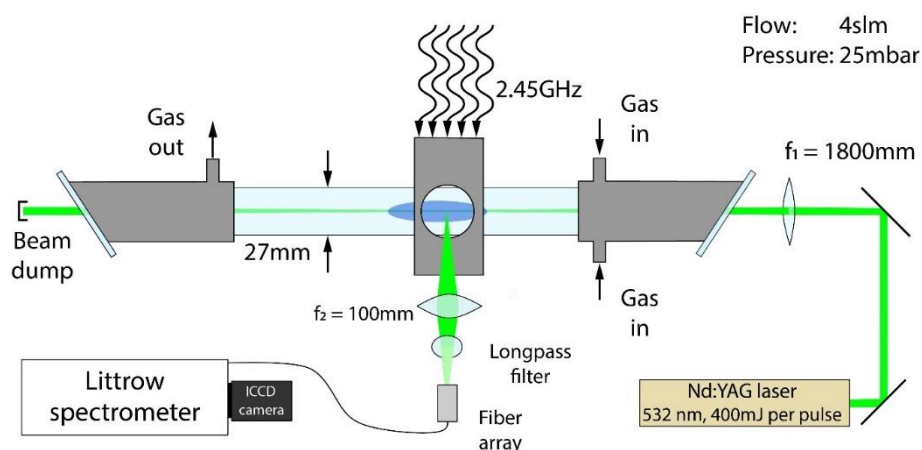

Figure 1: Schematic of the experimental setup used for these experiments, showing a vacuum system with a glass tube where the plasma is created, through the center of which a laser is focused to do laser scattering experiments. Scattered light is collected with a 100 mm focal distance lens and focused into a fiber array. A sharp-edge long-pass filter is placed in

Perfect impedance matching could not be realized for the entire duration of the plasma pulses due to variations in plasma impedance. These variations are caused by the increasing electron density, a relationship analyzed by Groen *et al.* [48], and observed in the works of Baeva *et al.* [49] & Golubovskii *et al.* [50]. A typical example of the changing absorbed power over time is shown in Figure 2.
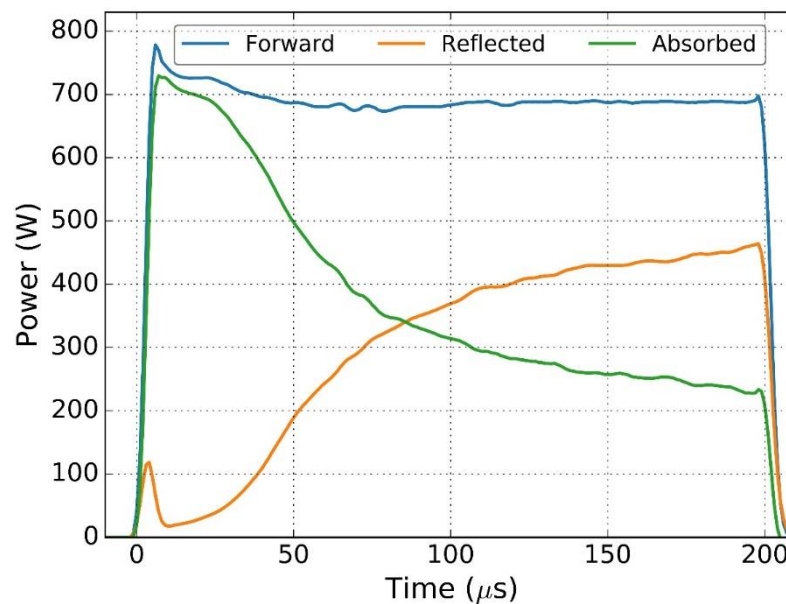

Figure 2: Example of measured forward and reflected microwave power and the resulting absorbed power. It illustrates the decreasing absorbed power as a result of degrading matching as plasma density builds up. Here, CO_2 plasma was ignited at 25 mbar and 4 slm.

The figure shows almost perfect tuning in the initial phases of the plasma with close to zero reflected power. As the electron density changes, the plasma impedance changes, the matching deteriorates and the reflected power increases. For all three gases, very similar power deposition profiles are obtained, which indicates plasma density building up similarly for different gases.

A 30 Hz, frequency doubled Nd:YAG laser (SpectraPhysics GCR-230) of 400 mJ per pulse is focused into the center of the plasma. A 100 mm focal distance lens collects and focuses the scattered light into a fiber array. The fibers relay the scattered light into a 50 μm entrance slit of a 1 m focal distance custom built Littrow-configuration spectrometer equipped with an 1800 l/mm grating, yielding a dispersion of 0.012 nm/pixel. The spectrally resolved image is captured by an em-ICCD (Princeton Instruments PiMax4) camera. More details on the general features of the experiment have been reported previously by Den Harder *et al.* [43].

Rejection of stray light and filtering of the Rayleigh light is crucial for resolving Thomson and Raman features. Both effects can be orders of magnitude stronger than Raman and Thomson scattering and need to be reduced to obtain a good signal-to-noise ratio. A sharp edge long-pass filter (Semrock RazorEdge) is used to block the laser frequency. The depolarized rotational Raman signal of CO_2 is used to calibrate the transmission of the filter, which results in the ability to measure electron temperatures as low as 1 eV.

A typical incoherent Thomson scattering spectrum measured in methane is shown in Figure 3. A threshold of 30% in transmittance is used to manually stop the fit around 533 nm. Spectral signature of products, most notably Laser Induced Fluorescence (LIF) from the Swan-bands of C_2 [51], is responsible for the structure on top of the Thomson signature, most visible at wavelengths larger than 536 nm. Since only a small spectral band can be observed, it is checked as follows that the measured signal is Thomson scattering signal and not produced by other means. Firstly, the polarization is confirmed to follow the laser polarization, thereby excluding LIF and Raman scattering. Secondly, it is confirmed that the signal disappears if either the camera gate is out-of-sync with the laser or when the plasma is off, thereby excluding plasma emission. Thirdly, the spectra are compared to measurements in a continuous argon discharge, in which spurious laser scattering contributions are absent. Electron densities are calibrated with the rotational Raman signal of nitrogen at room temperature and a pressure of 25 mbar, as described in [52].
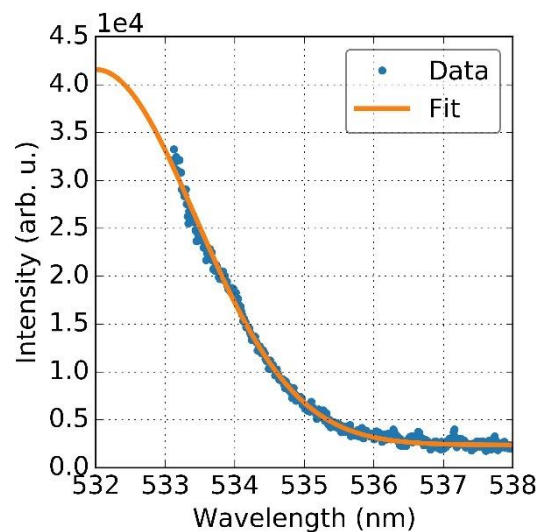

Figure 3: Thomson spectrum and Gaussian fit overlaid belonging to the 25 mbar, 4 slm CH_4 plasma at 100 µs into the pulse. The electron temperature for this spectrum is 1.9±0.2 eV. The electron density is $2.8 \pm 0.6 \cdot 10^{19} \ m^{-3}$.

Results & discussion
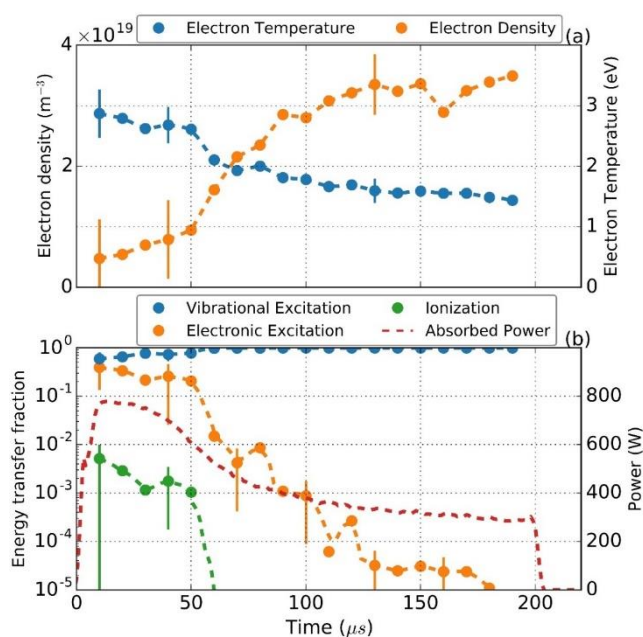
Plasma electron properties

Figure 4: (a) Electron temperature and density evolution measured by Thomson scattering in CH_4 plasma. (b) Power partitioning over vibrational and electronic excitation and ionization calculated on basis of the measured electron temperature with a Boltzmann solver (Bolsig+ [53]), taking cross sections from [54]. For comparison, also the measured absorbed power is shown. This figure shows the limited selectivity to vibrations during the onset of the pulse, where the input power is highest.

Evolutions of electron temperature and density in CH_4 plasma as measured with Thomson scattering are shown in Figure 4(a). The plot reveals that the electron temperature is decreasing from 2.8±0.4 eV to 1.4±0.2 eV over 200 μs. The electron density increases throughout the pulse while the plasma is developing towards its steady state conditions. It changes the impedance and consequently the matching, which explains the decreasing power absorption shown in Figure 6(b). In work on pulsed argon and nitrogen plasma these electron density trends are also observed and explained by the plasma density build up in the ionization phase [49][55].

The selectivity of electron energy transfer to vibrations is computed from the electron temperature measurements using a Boltzmann solver with a non-Boltzmann EEDF (Bolsig+ [56]) with cross sections from [54]. All vibrational modes of methane are lumped together, as are all the electronic states. The Thomson data provides a mean energy of the electrons coming from the standardly assumed Maxwell-Boltzmann distribution. It lacked sensitivity to give insight in the tail of the EEDF that is most important for estimating ionization and electron-impact dissociation. Therefore, the shape of the EEDF is calculated in the Boltzmann solver and, coupled with the T_e measured, used to

estimate the selectivity to different excitation channels. The result is shown in Figure 4(b) and illustrates how the initial high electron temperature limits the selectivity to vibrational activation during the plasma onset. A significant fraction of the input energy for the CH_4 plasma is deposited in electronic excitation: for 0<t<50 μs more than 10%. This inherently leads to dissociation since none of methane's electronic states are stable [57]. Moreover, it involves a significant reaction barrier that is converted into kinetic energy of the fragments and consequently heats the gas. The figure also shows that the strongest electron density increase occurs when the energy spent on ionization is already falling off. The changing absorbed power density is a likely explanation for this behavior. Alternatively, formation of carbon ions as main charge carrier may become important, which reduces charge recombination losses and consequently again the electron temperature and density [58]. The present diagnostic means do not allow to distinguish these effects unambiguously.

Resolving the Thomson scattering signatures is more challenging in N_2 and CO_2. The Thomson scattered light has a lower intensity than the Raman signal in the electron density regime that we have established for CH_4. In order to increase the sensitivity, we take advantage of the fact that the Thomson scattering signal is completely polarized whereas the rotational Raman signal is partly depolarized. Hence, the Raman signal can be eliminated by comparing the two polarizations of the scattered light and taking the depolarization ratio into account [46]. This approach consists of measuring two spectra at the same temporal and spatial position, but with perpendicular polarization. The spectrum following laser polarization contains both Raman and Thomson, whereas the perpendicularly polarized spectrum only contains Raman signal. Figure 5 illustrates this method and highlights the possibility to measure Thomson scattering in these molecular systems. The wing of the Thomson spectrum is fitted to a Gaussian profile to obtain the electron parameters: T_e = 1.8±0.6 eV and n_e = 1.0±0.5· 10^{19} m^{-3}.

The applicability of this technique depends on the ratio between Thomson and Raman signal strength. Only if the Raman signal does not exceed the Thomson signal by more than a factor of ~5, a reliable Thomson signature can be distinguished. The beneficial combination of high translational temperature, which lowers the neutral density and thus reduces the Raman contribution, and high electron density, which increases the Thomson signal, is achieved in our nitrogen discharges after 50 μs. Later in the pulse, in our case at $t > 80$ μs the plasma emission of the N_2 first positive system $\Delta v = -5$ [59] band becomes so strong that again the Thomson signature is blended.

So far, we have not succeeded to apply the same approach to CO_2 discharges. Firstly, the much larger rotational Raman cross section, which exceeds that of N_2 by a factor 9 [60], challenges the

sensitivity demands. Moreover, the more complicated and denser rotational spectrum prevented us to sufficiently resolve the rotational Raman structure for CO_2.
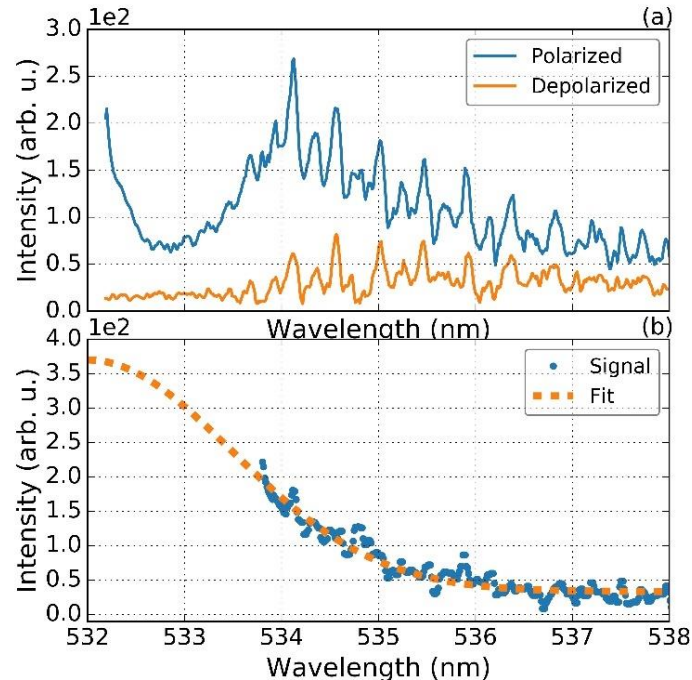

Figure 5: (a) The polarized and depolarized signals as measured in a pulsed N_2 discharge at t=50 μs, where the difference between signals represents the underlying Thomson signal. (b) The Thomson scattering signal as obtained after taking the filter response into account, where the cutoff wavelength of the filter is taken around 534nm as to not amplify the signal noise. The Gaussian fit yields T_e = 1.8±0.6 eV and $n_e = 1 \pm 0.5 \cdot 10^{19}$ m^{-3}. The slight asymmetry of the rotational Raman lines originates from the large population of vibrational states that have smaller rotational constants than the ground state.

Thomson scattering on CO_2 plasma in an argon background, one of the few works employing Thomson scattering in molecular systems, shows very similar electron temperature values as those detected in CH_4 and N_2 [61]. The electron parameters over the whole CO_2 pulse, as well as in N_2 for 0<t<50μs, where Thomson analysis was unsuccessful, are estimated on basis of those measured in CH_4. The estimates are based on the assumption of equal ionization frequency for the three discharge gases with the purpose of assessing the vibrational excitation selectivity for these gases. The equal ionization frequency is inspired by the similarity in electron loss frequencies (ambipolar diffusion and e-i recombination) as well as by experimentally observed power density and power-absorption curves. In CO_2 plasma this assumption is additionally supported by the similarity with CH_4 in electron-neutral collision frequency with E-fields between 40 Td and 100 Td (calculated with Bolsig+, cross sections from [62]), which is the range of electric fields expected in these pulsed plasmas. Of course, it is still only an assumption without true verification.

The resulting electron temperatures evolutions are shown in Figure 6(a), the vibrational excitation selectivity derived from those curves in Figure 6(b). Error margins are propagated from the CH_4 and N_2 electron temperature measurements.
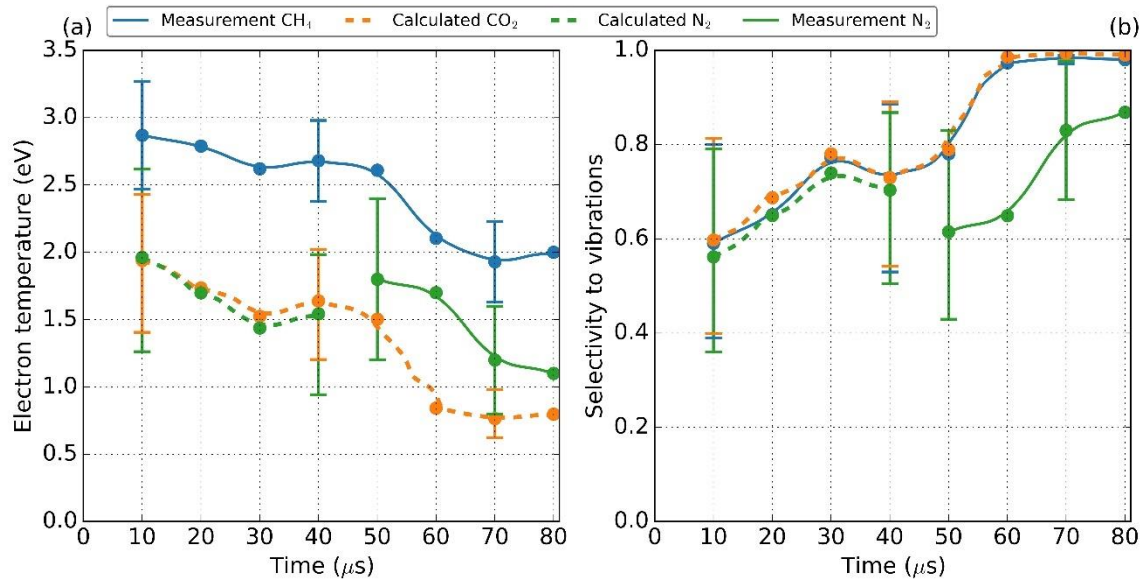

Figure 6: (a) Electron temperatures over time, measured (solid lines) for CH_4 and N_2, and calculated (dashed lines) from the CH_4 measurements for N_2 and CO_2. (b) The selectivity of power transfer to vibrations calculated with the electron temperatures in (a). Shown is an increasing selectivity as the pulse progresses, but also clearly indicated is a low selectivity during the discharge onset. All calculations were performed with Bolsig+ software [53], with cross sections from [54][62][63].

The results indicate very similar electron temperatures of CO_2 and N_2, while those of CH_4 are significantly higher. It is noteworthy to observe here that the computed and measured electron temperatures in N_2 plasma align well given the error margins. The calculated power partitioning shows the selectivity to be very similar for the three molecules: $\sim 60 \pm 20\%$ at the discharge onset up to $\sim 95 \pm 4\%$ after $80\,\mu s$ of the input energy is being transferred to CO_2 and CH_4 vibrations. The calculated power partitioning from the nitrogen measurements shows a lower selectivity: from $63 \pm 20\%$ after $40\,\mu s$ up to $87 \pm 10\%$ after $80\,\mu s$. After $80\,\mu s$, the selectivity remains above 90% for all cases. While the figure suggests excellent initial selectivity, we note that the error margins are significant. Consequently, the selectivity for CO_2, could be less than 50% up until t = $40\mu s$.

The remaining input energy fractions will mainly go into electronic excitation, as was detailed for CH_4 in Figure 4(b). Electronic excitation in nitrogen easily accumulates in its lowest electronic states, the metastable $A^3\Sigma_u^+$ and $a^1\Sigma_u^-$ states, because of their long radiative lifetimes (more than 10 s for A-state [64]). It means that an energy reservoir in the metastable states will build up over the pulse. For CO_2, the electronic excitation processes are not well characterized, but these will certainly play an important role in producing dissociation and accompanying gas heating. Our reasoning is that

dissociative electronic excitation involves a high energy threshold and thus is a channel that directly causes additional heat production via thermalization of the energetic dissociation products.

In conclusion, the power partitioning estimates on basis of the Thomson scattering measured electron temperatures indicate that initially 60±20% of the power is deposited in vibrations, a number that increases to ~90% at 80 μs. It also indicates that there is a significant fraction (>10%) of total energy spent in electronic excitation for all three molecules for t <50 μs. It is likely that most of this energy will end up in thermal heat through collisional quenching.

Heavy particle temperature dynamics

Vibrational temperatures are determined under the assumption that the vibrational levels are Boltzmann distributed. Only in N_2 plasma, and most pronounced in the early phase ($10\ \mu s < t <$ $50\ \mu s$), deviations from Boltzmann distribution were observed. In those cases, two vibrational temperatures were calculated: one for the ratio of ground and first excited state populations, $T_v^{0,1}$, and the other for the population distribution of all other observed vibrational bands, $T_v^{1,5}$, as described in [65][66]. Figure 7 shows such a deviation from a Boltzmann distribution as was typically measured in N_2, which is clearly significant for characterizing the energy stored in vibrational modes.
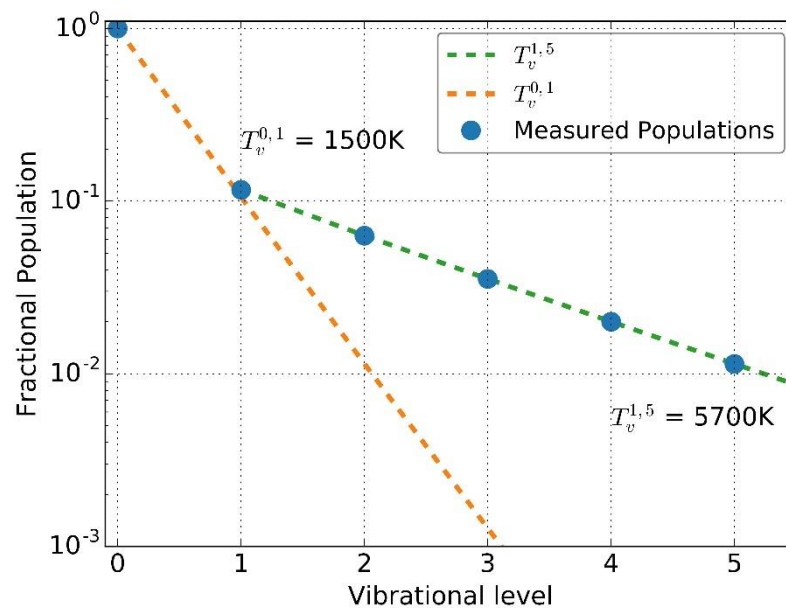

Figure 7: Boltzmann plot illustrating the bimodal vibrational distributions measured in the 25 mbar, 4 slm N_2 plasma at t=15 μs. $T_v^{0,1}$ is the usual Boltzmann temperature calculated from the ground state and first vibrational level population ratio. $T_v^{1,5}$ is the temperature describing the population distribution over the levels v=1-5. The two temperatures are respectively 1500 K and 5700 K.
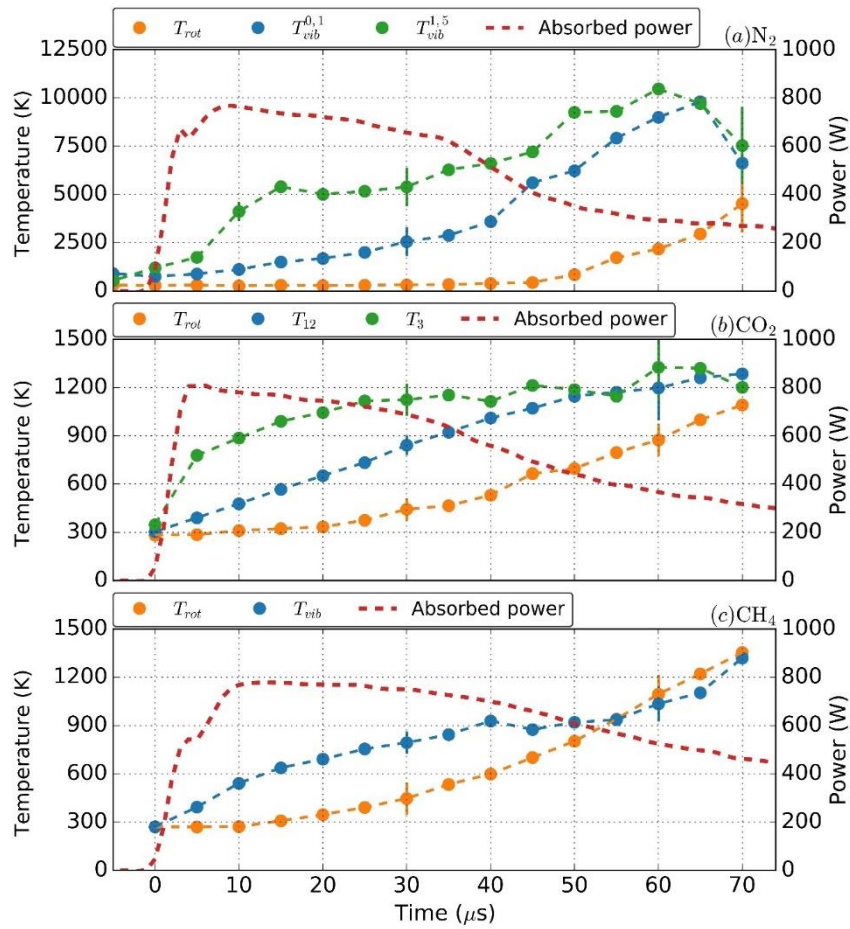
Figure 8: Rotational and vibrational temperature evolutions inferred from Raman scattering in the center of pulsed microwave plasmas of (a) N_2, (b) CO_2 and (c) CH_4. Deterioration of the coupling efficiency in the course of the pulse is reflected by the decreasing net absorbed power. Error bars shown for some representative data points are estimated from the quality of the Raman spectral fits and the signal-to-noise ratio. The large error in temperature for high rotational and vibrational temperatures in nitrogen is caused by low signal-to-noise ratios due to low scatter yields and a very low sensitivity to temperature of the first vibrational levels in the range of 10^4 K.

The heavy particle temperature evolutions in microwave discharges in N_2, CO_2 and CH_4 as inferred from Raman scattering measurements are shown in Figure 8. It is seen that the evolution of gas heating is significantly different for the three molecular systems. Nitrogen exhibits the largest vibrational excitation, with very limited initial gas heating. Moreover, it is the only molecule exhibiting a bimodal distribution, which can be observed from the start of the plasma. At the onset of the rapid gas heating in nitrogen this bimodal distribution disappears. The vibrational temperatures in N_2 reach almost 10000 K with a rotational temperature of less than 1000 K, whereas the vibrational temperatures measured for CO_2 and CH_4 are an order of magnitude lower. The

asymmetric stretching mode of CO_2 has initially the strongest increase, with T_3 reaching 1100 K at a gas temperature of 400 K. All vibrational modes equilibrate after 45 μs. This effect is not observed in CH_4, where all vibrational modes have equal temperature throughout the discharge, confirming the strong coupling between all its vibrational modes. The evolution of T_{12} in CO_2 is very similar to that of T_{vib} in CH_4: The maximum difference between T_{12}/T_{vib} and T_{rot} is about 300 K. The much higher vibrational temperatures in N_2 must be evaluated in the context of its smaller vibrational heat capacity; N_2 only has one vibrational mode, whereas CO_2 has four and CH_4 has nine (including degeneracies). The vibrational heat capacities for each molecule are evaluated following the approach of our earlier work on CO_2 [44] using

$$c_{\text{p,vib}} = \sum_i d_i z_i \left(\frac{\ln(z_i)}{1 - z_i} \right)^2 R. \qquad \textit{eq. 1}$$

Here d_i is the degeneracy of mode i, z_i is the typical Boltzmann term associated with this mode, expressed as $z_i = \exp(hc\omega_i/kT_i)$, and R is the gas constant. For the low vibrational temperatures observed in CO_2 and CH_4 the Boltzmann terms have not yet reached their maximum value, while N_2, reaching a T_{vib} of 10000 K does reach its maximum heat capacity. Hence the high vibrational temperature of N_2 holds significantly more energy than the vibrational energies in all the modes of CO_2 and CH_4: 10000K T_{vib} in N_2 holds the same energy as 2075 K in CH_4 and 2850 K in CO_2.

In gas temperature evolution, CH_4 and CO_2 are similar, but different compared with nitrogen. Where the temperature in CO_2 and CH_4 rises gradually to 1000-1300 K over the entire 70 μs pulse duration, there is almost no change in gas temperature in N_2 for 40 μs, after which the temperature rises rapidly to more than 3000 K at 70 μs. This increase in N_2 will lead to thermalization shortly after 70 μs, which could not directly be measured due to the abruptly dropping Raman intensity. The rapid gas heating after 50 μs is also observed in recent work on N_2 pulsed microwave plasma [67], where the gas heating stops at around 1000 K and the non-equilibrium is sustained.

An interesting point of discussion is the actual amount of vibrational driven dissociation occurring in the three studied plasmas, something difficult to quantify without extensive state-to-state models. However, on basis of the population fractions in the asymmetric stretching mode for CO_2 and CH_4 we can argue that it is minimal: for successful vibrational-driven dissociation a significant fraction of molecules must have one or more quanta in this vibrational mode. The population fractions in this mode only reach $\sim$5%, which likely is not sufficient to overcome the losses to other vibrational modes occurring at higher vibrational levels. For N_2 this is not the case, as there is only one mode of vibration that reaches much higher temperatures and population fractions. However, only N-atoms can be formed, which readily recombine so that no net chemistry can occur.

Having established the heating dynamics of vibrational and gas kinetic modes, we shall analyze the heat equilibration via VT relaxation involving parent molecules as well as dissociation products for each of the three molecules.

Nitrogen

The observed rapid heating in the nitrogen plasma could typically be explained by a vibrational or thermal instability [68], in which the large amount of energy stored in the molecule's vibrations quickly relaxes due to the positive feedback loop between VT relaxation and temperature. However, the VT timescales for pure N_2 are orders of magnitude longer than the pulse length for the temperature regime under discussion: at 750 K the typical VT time in N_2 is 400 ms [19]. Clearly, the heat generation at $t > 50 \, \mu$s must be caused by other processes than molecular VT relaxation. An efficient and well-studied thermalization mechanism in N_2 plasma is N_2-N VT relaxation [17][69][70]. Nitrogen atoms are much more efficient in quenching metastable vibrational (and electronic) states than molecular nitrogen and have consequently often been identified to play a key part in heating N_2 plasma. The rates of N_2-N VT relaxation are non-zero above v=10 and rise rapidly with both higher quantum number and gas temperature [32]. The relevance of this heating channel in our particular plasma is assessed based on N concentration measurements.

The atomic nitrogen concentration is estimated following the method described by Coitout *et al.* [71]. It involves measurements of the decay rate of the Second Positive System (SPS) afterglow emission. In the afterglow, where no energetic electrons exist, the main population channel of the radiative N_2 $(C^3\Pi_u)$ state is the pooling reaction:

$$N_2 \, (A^3\Sigma_u^+) + N_2 (A^3\Sigma_u^+) \rightarrow N_2(C^3\Pi_u) + N_2(X^1\Sigma_g). \qquad \textit{eq. 2}$$
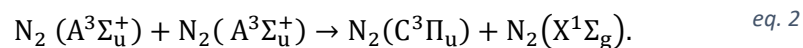
In the afterglow there is no excitation of the N_2 $(A^3\Sigma_u^+)$ state while quenching occurs predominantly by atomic nitrogen. Quenching of $N_2(A^3\Sigma_u^+)$ reduces the production of $N_2(C^3\Pi_u)$ and thus the emission intensity of the SPS. The results of the model presented by Coitout *et al.* are used to convert the measurements of afterglow decay rate into atomic nitrogen concentration. This model couples the N_2 $(C^3\Pi_u)$, $(B^3\Pi_g)$, $(A^3\Sigma_u^+)$ and $(X^1\Sigma_g)$ states as well as the N density through radiative transfers, pooling reactions, quenching and collisional transfer. It yields a straightforward way of obtaining N densities from the $N_2(C^3\Pi_u)$ radiative decay.
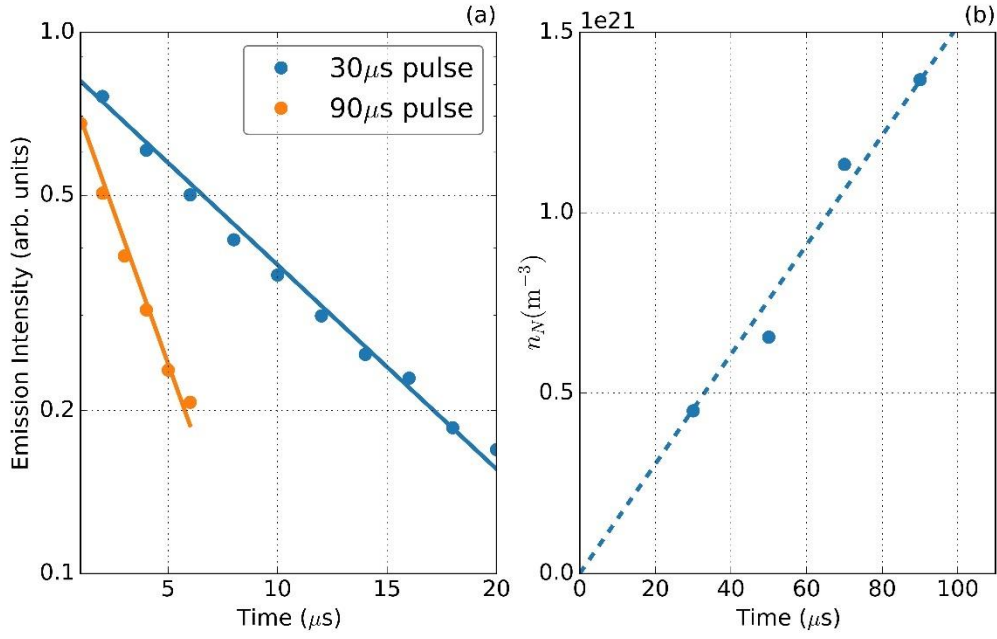
Figure 9: (a) The decay of the SPS emission measured in the afterglow for a plasma pulse duration of 90 μs and 30 μs, respectively. (b) The absolute density of atomic nitrogen computed from the SPS emission decay as a function of plasma pulse duration. An increase in nitrogen atom density is clearly observed throughout the pulse.

Figure 9(a) shows the emission intensity in the afterglow for a 30 and 90 μs plasma, clearly exhibiting a faster decay for longer pulses. The atomic N density obtained from the decay rates is shown in Figure 9(b). These, together with the vibrational and gas temperatures, enable us to quantify the heat coming from N_2-N VT reactions. The high vibrational levels (10<v<40) are most important for these reactions as shown in [17]. However, these levels are not directly measurable due to their relatively small population. Hence the same VDF as in the work of Guerra *et al.* (ref [17], fig. 4a) is assumed, since the gas temperature and vibrational temperatures are very similar before the heating commences. The atomic N density in this calculation is set at 10^{21} m^{-3}, corresponding to a dissociation fraction of ~1%. The energy leaving vibrational modes per volume per second, or the vibrational cooling, is computed as:

$$P_{VT} = \sum_v \sum_{v'} [N_2(v)]\,[N]\,k_{v,v'}\Delta E_{v,v'}. \qquad \text{\textit{eq. 3}}$$

Here, $[N_2(v)]$ is the density of N_2 vibrational state v, [N] is the atomic N density, $k_{v,v'}$ is the rate for the specific collision from $N_2(v)$ to $N_2(v')$, calculated with the equations described in [32] for 1000 K, and $\Delta E_{v,v'}$ is the energy that is lost to heat in such a collision. Finally, the vibrational cooling rate is assumed equal to the gas heating rate. This calculation results in a gas heating rate of 25 Kμs^{-1}, which is to be compared with the observed ~100 Kμs^{-1} (Figure 8). Given the uncertainties in the

analysis that come mainly from the estimated atomic N density and details of the VDF, we conclude that atomic N formation and its subsequent quenching of internally excited N_2 dominates the gas heating in N_2 plasma.

Methane

The equilibration timescale of T_{vib} and T_{rot} in CH_4 is close to the characteristic timescale of VT relaxation at 25 mbar and 300 K, which was reported to be 50 μs [20], suggesting VT relaxation to dominate at forehand. We compute the vibrational cooling as [37]:

$$-\frac{dE_{vib}}{dt} = \frac{dE_{gas}}{dt} = \frac{1}{\tau_{VT}}\left(E_{vib}(T_{vib}) - E_{vib}(T_{gas})\right) \qquad \textit{eq. 4}$$

Here, $E_{vib}(T_{vib})$ is the energy in vibrations, evaluated at the measured vibrational temperature and $E_{vib}(T_{gas})$ the energy in vibrations if the gas was in equilibrium. Furthermore, the temperature dependent VT relaxation, τ_{VT}, is described by a general scaling relation:

$$\log_{10}(\tau_{VT}\,p) = \left(a\,T^{\frac{1}{3}} - b\right). \qquad \textit{eq. 5}$$

Here, a and b are experimentally determined coefficients, T is the temperature in K, and p is the pressure in bar. Temperature dependent VT times are taken from Wang & Springer [72]. The result is shown in Figure 10.
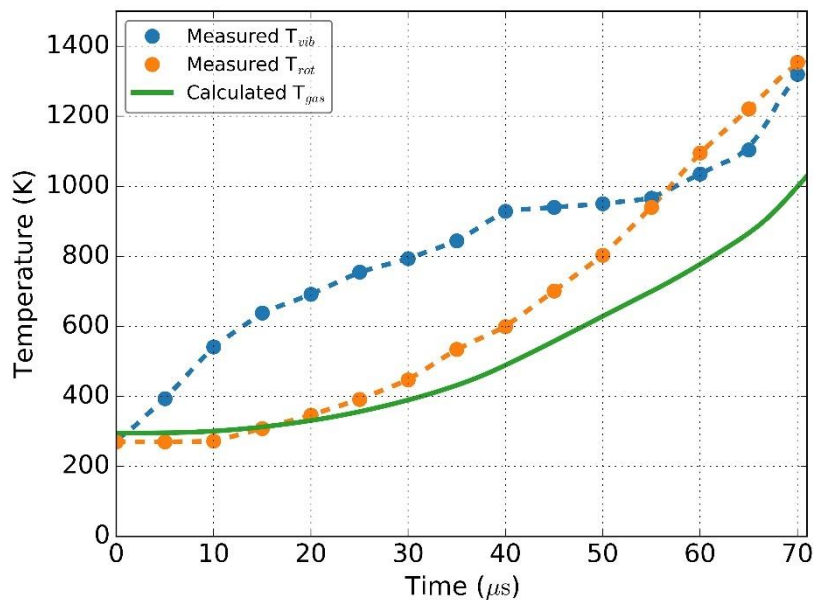

Figure 10: Gas heating from VT relaxation calculated for methane on basis of the measured vibrational temperature evolutions as a function of time. It confirms that VT relaxation in CH_4-CH_4 collisions is the dominant heating mechanism.

The figure shows an underestimation of the calculated gas temperature compared to the measurements, which increases to about 300 K after 70 μs. Nevertheless, 70% of the observed temperature rise can be attributed to VT relaxation. The remaining heating is probably induced via energetic dissociative excitation products, which amounts to 20$\pm$5% of the power input throughout the pulse. Moreover, the dissociation products and resulting higher hydrocarbons quench methane vibrational excitation even more efficiently, underlining another complicating factor for vibrational chemistry in CH_4 plasma. Particularly ethane, identified as one of the main reaction products [36], quenches the vibrations of CH_4 resonantly [41]. For example, 0.5% ethane concentration shortens VT times by approximately a factor 40.

Bolsig+ calculations were performed, which indicate that lowering the electron temperature for CH_4 during ignition will lead to more power being deposited in the vibrational modes of CH_4, and thus to a higher vibrational temperature. The time limitations of VT relaxation in a 100% selective case were estimated by running the calculation of Figure 10 with a 50% higher vibrational temperature. This results in an equilibration time of 50 μs, thereby showing that VT relaxation would limit vibrational non-equilibrium in CH_4 plasma even if 100% selectivity were achieved.

Carbon dioxide

The importance of VT relaxation for gas heating in CO_2 is analyzed similarly as for CH_4. State-to-state mechanics are ignored and the overall VT relaxation is computed by assuming one vibrational temperature and one VT rate, like in work by Simpson *et al.* [16] and Carnevale *et al.* [37]. Complicating in this approach is our observation of the different temperatures for the asymmetric versus the bending and symmetric stretch vibrations. We simply ignore the higher temperature of the asymmetric stretch mode and the complexities in VV and VT transfer arising from it. This is justified by the relatively small amount of energy contained in the asymmetric stretch mode, an observation made in our previous work reported by Van den Bekerom *et al.* [44].

The CO_2 VT times as a function of temperature are calculated using the fitting coefficients of Simpson *et al.* [73]. Figure 11 shows the result of the calculation for CO_2 in a comparison with the measured temperatures. It is noted that the parameters established in Carnevale *et al.* [37] yield similar results.
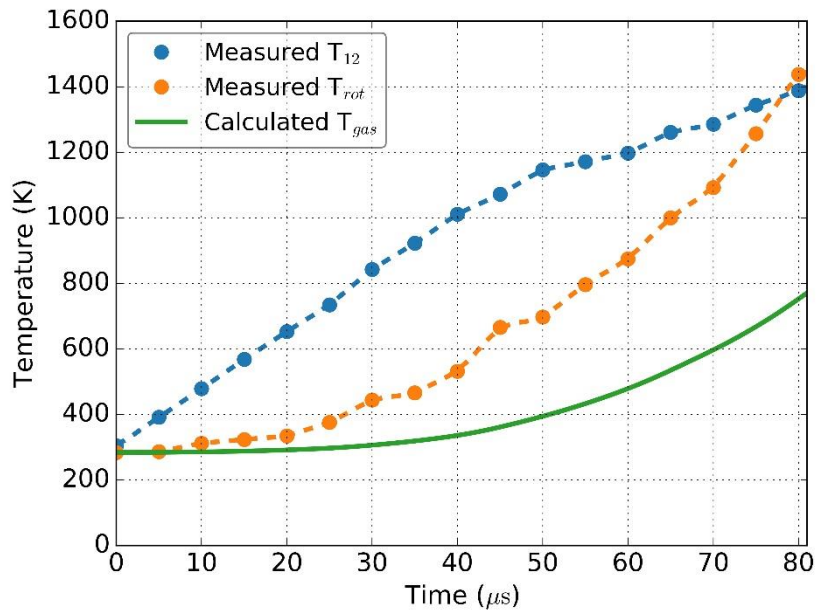
Figure 11: VT relaxation in CO_2 simulated for the measured T_{12} trace. T_3 is not shown since it is not being considered in this calculation. Comparison with the measurement of the rotational temperature shows that the simulated gas heating is ~50% slower than in the experiment.

Comparison of the simulated VT relaxation with the observed gas heating shows that the simulation underestimates the gas heating time constant by ~50%. Dissociation products in CO_2 plasma may shorten effective VT times, similar as was discussed for CH_4 and N_2. Atomic oxygen is approximately an order of magnitude more potent in quenching vibrations than CO_2 itself [38]. Still, a dissociation fraction of ~10% is required to decrease the effective VT times sufficiently to correctly predict the measured gas temperatures. Such degree of dissociation is not reached since no spectral features of products are seen in the rotational Raman measurements: atomic oxygen Raman lines at 158 cm^{-1} and 226 cm^{-1} Raman shift [74], seen in continuous CO_2 plasma, were not observed. Dedicated efforts to measure the vibrational Raman signature of CO also proved fruitless. Both spectral signatures would lie within the detection limit of the system, which is around 5% at these conditions, indicating the low degree of dissociation locally.

While product-accelerated VT-relaxation does not contribute significantly to gas heating, the formation of products can be significant: electron-impact excitation and dissociation release significant heat per reaction. This channel is therefore concluded to generate the remaining heat, a conclusion that is in line with the selectivity assessment of Figure 6, where up to 50% of electron energy could be spent in electronic excitation initially.

19

General conclusions

Pulsed microwave plasma was studied for efficient reforming of the stable and abundant molecules: N_2, CH_4, and CO_2. Electron, vibrational and rotational temperatures, measured by Thomson and Raman scattering, were used to obtain a detailed insight in the heating dynamics in the breakdown phase of these microwave plasmas. Strong vibrational non-equilibria were observed during this phase of the discharge. Despite differences in energy transfer mechanisms and mode equilibration timescales, all three gases were observed to heat up within 0.1 ms.

The electron temperature in methane and nitrogen plasma were observed to decrease over time, from 2.8 to 1.4 eV in the case of CH_4 and from 1.8 to 1.1 eV in N_2. Where no Thomson signature was observed, the time trace of the electron temperatures in CO_2 and N_2 was estimated by assuming similar ionization frequencies. These electron temperatures are too high for preferential vibrational excitation in N_2, CO_2 and CH_4, and indicate that 10-40% of the input energy is transferred to electronic excitation in all three gases in the first 50 μs of the pulse.

Dissociation products are generally efficient vibrational quenchers. O, N, and C_2H_6 are all efficient in quenching vibrations of their parent molecules. This is the main heating mechanism in the nitrogen plasma, where nitrogen atoms were identified as cause for the observed gas heating. For CO_2 and CH_4, no significant product formation could be observed within the duration of the plasma pulse to see effect on the gas heating.

On basis of these considerations, we generalize the promises and limitations of vibrationally driven plasma chemistry. In our experiments, the non-equilibrium was always limited to less than 100 μs. It is noted that reactor pressure and power density govern the timescale for relaxation and gas heating. Lowering the pressure will extend the timescale but will also impact the timescales of transport and chemistry. Nitrogen already shows very promising results under the present conditions, with high vibrational temperatures and significant dissociation. Here the challenge will be in separating the excitation and dissociation, as to prevent the quenching through product formation. For CO_2, control of the electron temperature would be a solution for a longer lasting and more significant non-equilibrium. In CH_4 we observed that VT relaxation is the dominant heating mechanism, which can only be suppressed by actively cooling the gas. Perhaps more sophisticated approaches could negate the identified limitations and broaden the window of opportunity for vibrational excitation. These include the aforementioned sodium seeding to increase electron densities and e-V selectivity as well as plasma ignition in a supersonic expansion to actively cool the gas.

Conflicts of interest

There are no conflicts of interest to declare

Acknowledgements

References

[1]   A. Bogaerts and E. C. Neyts, "Plasma Technology: An Emerging Technology for Energy Storage," *ACS Energy Lett.*, vol. 3, no. 4, pp. 1013–1027, 2018, doi: 10.1021/acsenergylett.8b00184.

[2]   P. Mehta *et al.*, "Overcoming ammonia synthesis scaling relations with plasma-enabled catalysis," *Nat. Catal.*, vol. 1, no. 4, pp. 269–275, 2018, doi: 10.1038/s41929-018-0045-1.

[3]   T. Nozaki, N. Muto, S. Kado, and K. Okazaki, "Dissociation of vibrationally excited methane on Ni catalyst: Part 1. Application to methane steam reforming," *Catal. Today*, vol. 89, no. 1–2, pp. 57–65, 2004, doi: 10.1016/j.cattod.2003.11.040.

[4]   L. Chen, J. A. Lau, D. Schwarzer, J. Meyer, V. B. Verma, and A. M. Wodtke, "The Sommerfeld ground-wave limit for a molecule adsorbed at a surface," *Science (80-.).*, vol. 363, no. 6423, pp. 158–161, 2019, doi: 10.1126/science.aav4278.

[5]   C. E. Treanor, J. W. Rich, and R. G. Rehm, "Vibrational Relaxation of Anharmonic Oscillators with Exchange-Dominated Collisions," *J. Chem. Phys.*, vol. 48, no. 4, pp. 1798–1807, 1968, doi: 10.1063/1.1668914.

[6]   P. Capezzuto, F. Cramarossa, R. D'Agostino, and E. Molinari, "Contribution of vibrational excitation to the rate of carbon dioxide dissociation in electrical discharges," *J. Phys. Chem.*, vol. 80, no. 8, pp. 882–888, 1976, doi: 10.1021/j100549a024.

[7]   A. Bogaerts, T. Kozak, K. van Laer, and R. Snoeckx, "Plasma-based conversion of CO 2 : current status and future challenges," *Faraday Discuss.*, vol. 183, pp. 217–232, 2015, doi: 10.1039/c5fd00053j.

[8]   Y. P. Butylkin *et al.*, "Dissociation of CO2 by a plasma-chemical process in a nonequilibrium microwave discharge," *Sov. Phys. Tech. Phys.*, vol. 26, no. 5, pp. 555–558, 1981.

[9]   V. D. Rusanov, A. A. Fridman, and G. V. Sholin, "The Physics of a Chemically Active Plasma with nonequilibrium vibrational excitation of molecules," *Sov. Phys. Usp.*, vol. 24, no. 6, pp. 185–235, 1981.

[10]   P. Diomede, M. C. M. Van De Sanden, and S. Longo, "Insight into CO2 Dissociation in Plasma from Numerical Solution of a Vibrational Diffusion Equation," *J. Phys. Chem. C*, vol. 121, no. 36, pp. 19568–19576, 2017, doi: 10.1021/acs.jpcc.7b04896.

[11]   T. Kozàk and A. Bogaerts, "Splitting of CO2 by vibrational excitation in non-equilibrium plasmas: A reaction kinetics model," *Plasma Sources Sci. Technol.*, vol. 23, no. 4, 2014, doi: 10.1088/0963-0252/23/4/045004.

[12]   A. Fridman, *Plasma chemistry*, 1st ed., vol. 9780521847. Cambridge University Press, 2008.

[13]   T. Nozaki and K. Okazaki, "Non-thermal plasma catalysis of methane: Principles, energy efficiency, and applications," *Catal. Today*, vol. 211, pp. 29–38, 2013, doi: 10.1016/j.cattod.2013.04.002.

[14]   Y. Itikawa, "Cross sections for electron collisions with carbon dioxide," *J. Phys. Chem. Ref. Data*, vol. 31, no. 3, pp. 749–767, 2002, doi: 10.1063/1.1481879.

[15]   R. Snoeckx and A. Bogaerts, "Plasma technology-a novel solution for CO2 conversion?," *Chem. Soc. Rev.*, vol. 46, no. 19, pp. 5805–5863, 2017, doi: 10.1039/c6cs00066e.

[16]   C. J. S. M. Simpson, K. B. Bridgman, and T. R. D. Chandler, "Shock-tube study of vibrational relaxation in carbon dioxide," *J. Chem. Phys.*, vol. 49, no. 2, pp. 513–522, 1968, doi: 10.1063/1.1670105.

[17]   V. Guerra, E. Tatarova, F. M. Dias, and C. M. Ferreira, "On the self-consistent modeling of a traveling wave sustained nitrogen discharge," *J. Appl. Phys.*, vol. 91, no. 5, pp. 2648–2661, 2002, doi: 10.1063/1.1446229.

[18]   B. F. Gordiets and S. Zhdanok, "Analytical Theory of Vibrational Kinetics of Anharmonic Oscillators," in *Nonequilibrium vibrational kinetics*, 1986, pp. 47–84.

[19]   V. Blackman, "Vibrational relaxation in oxygen and nitrogen," *J. Fluid Mech.*, vol. 1, no. 1, pp. 61–85, 1956, doi: 10.1017/S0022112056000056.

[20]   M. H. Cabral, "Vibrational Relaxation Times in Methane," University of Amsterdam, 1976.

[21]   Y. Gan, C. Liang, C. Hamel, H. Cutforth, and H. Wang, "Strategies for reducing the carbon footprint of field crops for semiarid areas. A review," *Agron. Sustain. Dev.*, vol. 31, no. 4, pp.

643–656, 2011, doi: 10.1007/s13593-011-0011-7.

[22]   C. De Bie, B. Verheyde, T. Martens, J. Van Dijk, S. Paulussen, and A. Bogaerts, "Fluid modeling of the conversion of methane into higher hydrocarbons in an atmospheric pressure dielectric barrier discharge," *Plasma Process. Polym.*, vol. 8, no. 11, pp. 1033–1058, 2011, doi: 10.1002/ppap.201100027.

[23]   M. Heintze, M. Magureanu, and M. Kettlitz, "Mechanism of C2 hydrocarbon formation from methane in a pulsed microwave plasma," *J. Appl. Phys.*, vol. 92, no. 12, pp. 7022–7031, 2002, doi: 10.1063/1.1521518.

[24]   B. L. M. Klarenaar, R. Engeln, D. C. M. Van Den Bekerom, M. C. M. Van De Sanden, A. S. Morillo-Candas, and O. Guaitella, "Time evolution of vibrational temperatures in a CO2 glow discharge measured with infrared absorption spectroscopy," *Plasma Sources Sci. Technol.*, vol. 26, no. 11, 2017, doi: 10.1088/1361-6595/aa902e.

[25]   T. Silva *et al.*, "Kinetic study of low-temperature CO2 plasmas under non-equilibrium conditions. I. Relaxation of vibrational energy," *Plasma Sources Sci. Technol.*, vol. 27, no. 1, 2018, doi: 10.1088/1361-6595/aaa56a.

[26]   G. Trenchev, A. Nikiforov, W. Wang, S. Kolev, and A. Bogaerts, "Atmospheric pressure glow discharge for CO2 conversion: Model-based exploration of the optimum reactor configuration," *Chem. Eng. J.*, vol. 362, no. October 2018, pp. 830–841, 2019, doi: 10.1016/j.cej.2019.01.091.

[27]   D. C. M. van den Bekerom *et al.*, "The importance of thermal dissociation in CO2 microwave discharges investigated by power pulsing and rotational Raman scattering," *Plasma Sources Sci. Technol.*, vol. 28, no. 5, 2019, doi: 10.1088/1361-6595/aaf519.

[28]   G. J. Van Rooij *et al.*, "Taming microwave plasma to beat thermodynamics in CO2 dissociation," *Faraday Discuss.*, vol. 183, pp. 233–248, 2015, doi: 10.1039/c5fd00045a.

[29]   A. Vesel, M. Mozetic, A. Drenik, and M. Balat-Pichelin, "Dissociation of CO2 molecules in microwave plasma," *Chem. Phys.*, vol. 382, no. 1–3, pp. 127–131, 2011, doi: 10.1016/j.chemphys.2011.03.015.

[30]   W. Bongers *et al.*, "Plasma-driven dissociation of CO2 for fuel synthesis," *Plasma Process. Polym.*, vol. 14, no. 6, pp. 1–8, 2016, doi: 10.1002/ppap.201600126.

[31]   A. Ricard, S. G. Oh, J. Jang, and Y. K. Kim, "Quantitative evaluation of the densities of active species of N2 in the afterglow of Ar-embedded N2 RF plasma," *Curr. Appl. Phys.*, vol. 15, no.

11, pp. 1453–1462, 2015, doi: 10.1016/j.cap.2015.08.013.

[32]   V. Guerra, A. Tejero-del-Caz, C. D. Pintassilgo, and L. L. Alves, "Modelling N 2 –O 2 plasmas: volume and surface kinetics," *Plasma Sources Sci. Technol.*, vol. 28, no. 7, 2019, doi: 10.1088/1361-6595/ab252c.

[33]   N. Gatti *et al.*, "Preferential vibrational excitation in microwave nitrogen plasma assessed by Raman scattering," *Plasma Sources Sci. Technol.*, vol. 27, no. 5, 2018, doi: 10.1088/1361-6595/aabd60.

[34]   Y. Xu, X. Bao, and L. Lin, "Direct conversion of methane under nonoxidative conditions," *J. Catal.*, vol. 216, pp. 386–395, 2003, doi: 10.1016/S0021-9517(02)00124-0.

[35]   R. Horn and R. Schlögl, "Methane Activation by Heterogeneous Catalysis," *Catal. Letters*, vol. 145, no. 1, pp. 23–39, 2015, doi: 10.1007/s10562-014-1417-z.

[36]   T. Minea *et al.*, "Non-oxidative methane coupling to C2 hydrocarbons in a microwave plasma reactor," *Plasma Process. Polym.*, vol. 15, no. 11, pp. 1–16, 2018, doi: 10.1002/ppap.201800087.

[37]   E. H. Carnevale, C. Carey, and G. Larson, "Ultrasonic determination of rotational collision numbers and vibrational relaxation times of polyatomic gases at high temperatures," *J. Chem. Phys.*, vol. 47, no. 8, pp. 2829–2835, 1967, doi: 10.1063/1.1712305.

[38]   R. E. Center, "Vibrational relaxation of CO2 by O atoms," *J. Chem. Phys.*, vol. 59, no. 7, pp. 3523–3527, 1973, doi: 10.1063/1.1680514.

[39]   C. B. Moore, R. E. Wood, B. L. Hu, and J. T. Yardley, "Vibrational energy transfer in CO2 lasers," *J. Chem. Phys.*, vol. 46, no. 11, pp. 4222–4231, 1967, doi: 10.1063/1.1840527.

[40]   A. J. Demaria, "Review of CW High-Power CO2 lasers," *Proc. IEEE*, vol. 61, no. 6, pp. 731–748, 1973, doi: 10.1017/CBO9781107415324.004.

[41]   J. T. Yardley, M. N. Fertig, and C. Bradley Moore, "Vibrational deactivation in methane mixtures," *J. Chem. Phys.*, vol. 52, no. 3, pp. 1450–1453, 1970, doi: 10.1063/1.1673149.

[42]   J. T. Yardley and C. Bradley Moore, "Vibrational energy transfer in methane," *J. Chem. Phys.*, vol. 49, no. 3, pp. 1111–1125, 1968, doi: 10.1063/1.1670199.

[43]   N. den Harder *et al.*, "Homogeneous CO2 conversion by microwave plasma: Wave propagation and diagnostics," *Plasma Process. Polym.*, vol. 14, no. 6, pp. 1–24, 2017, doi: 10.1002/ppap.201600120.

[44]   D. van den Bekerom, A. van de Steeg, R. Van de Sanden, and G. J. Van Rooij, "Mode resolved heating dynamics in pulsed microwave CO2 plasma from laser Raman scattering," *J. Phys. D. Appl. Phys.*, p. in press, 2019, doi: 10.1088/1361-6463/ab5311.

[45]   M. Ramakers, I. Michielsen, R. Aerts, V. Meynen, and A. Bogaerts, "Effect of Argon or Helium on the CO 2 Conversion in a Dielectric Barrier Discharge," pp. 755–763, doi: 10.1002/ppap.201400213.

[46]   D. A. Long, *Raman Spectroscopy*, 1st ed. McGraw-Hill International Book Company, 1977.

[47]   T. D. Butterworth *et al.*, "Quantifying methane vibrational and rotational temperature with Raman scattering," *J. Quant. Spectrosc. Radiat. Transf.*, vol. 236, p. 106562, 2019, doi: 10.1016/j.jqsrt.2019.07.005.

[48]   P. W. C. Groen, A. J. Wolf, T. W. H. Righart, M. C. M. Van De Sanden, F. J. J. Peeters, and W. A. Bongers, "Numerical model for the determination of the reduced electric field in a CO2 microwave plasma derived by the principle of impedance matching," *Plasma Sources Sci. Technol.*, vol. 28, no. 7, 2019, doi: 10.1088/1361-6595/ab1ca1.

[49]   M. Baeva *et al.*, "Experimental study of pulsed microwave discharges in nitrogen," *Plasma Sources Sci. Technol.*, vol. 8, no. 1, pp. 142–150, 1999, doi: 10.1088/0963-0252/8/1/017.

[50]   Y. B. Golubovskii, R. V. Kozakov, V. A. Maiorov, A. V. Meshchanov, I. A. Porokhova, and A. Rousseau, "Dynamics of gas heating in a pulsed microwave nitrogen discharge at intermediate pressures," *J. Phys. D. Appl. Phys.*, vol. 37, no. 6, pp. 868–874, 2004, doi: 10.1088/0022-3727/37/6/011.

[51]   P. E. Bengtsson and M. Aldén, "C2 Production and Excitation in Sooting Flames using Visible Laser Radiation: Implications for Diagnostics in Sooting Flames," *Combust. Sci. Technol.*, vol. 77, pp. 307–318, 1991, doi: 10.1080/00102209108951733.

[52]   E. A. D. Carbone, S. Hübner, J. M. Palomares, and J. J. A. M. Van Der Mullen, "The radial contraction of argon microwave plasmas studied by Thomson scattering," *J. Phys. D. Appl. Phys.*, vol. 45, no. 34, 2012, doi: 10.1088/0022-3727/45/34/345203.

[53]   "http://www.bolsig.laplace.univ-tlse.fr/." .

[54]   W. L. Morgan, "A critical evaluation of low-energy electron impact cross sections for plasma processing modeling. II: Cl4, SiH4, and CH4," *Plasma Chem. Plasma Process.*, vol. 12, no. 4, pp. 477–493, 1992, doi: 10.1007/BF01447255.

[55] S. Hübner, J. M. Palomares, E. A. D. Carbone, and J. J. A. M. Van Der Mullen, "A power pulsed low-pressure argon microwave plasma investigated by Thomson scattering: Evidence for molecular assisted recombination," *J. Phys. D. Appl. Phys.*, vol. 45, no. 5, 2012, doi: 10.1088/0022-3727/45/5/055203.

[56] "MORGAN database, http://www.lxcat.laplace.univ-tlse.fr, retrieved June 4, 2013." .

[57] M. Y. Song *et al.*, "Cross sections for electron collisions with methane," *J. Phys. Chem. Ref. Data*, vol. 44, no. 2, 2015, doi: 10.1063/1.49 18630.

[58] T. Minea *et al.*, "Role of Electron–Ion Dissociative Recombination in CH 4 Microwave Plasma on Basis of Simulations and Measurements of Electron Energy," *Plasma Chem. Plasma Process.*, vol. 39, no. 5, pp. 1275–1289, 2019, doi: 10.1007/s11090-019-10005-w.

[59] M. Simek, G. Dilecce, and S. Benedictis, "On the use of numerical simulations of the first positive system of N2: I. Emission and LIF analysis," *Plasma Chem. Plasma Process.*, vol. 15, no. 3, pp. 427–449, 1995.

[60] C. M. Penney, R. L. St. Peters, and M. Lapp, "Absolute Rotational Raman Cross Sections for N2, O2 and CO2.," *J. Opt. Soc. Am.*, vol. 64, no. 5, pp. 712–716, 1974, doi: 10.1364/JOSA.64.000712.

[61] S. Hübner, E. Carbone, J. M. Palomares, and J. Van Der Mullen, "Afterglow of argon plasmas with H2, O2, N 2, and CO2 admixtures observed by thomson scattering," *Plasma Process. Polym.*, vol. 11, no. 5, pp. 482–488, 2014, doi: 10.1002/ppap.201300190.

[62] Http://www.lxcat.laplace.univ-tlse.fr, "MORGAN database." .

[63] A. V. Vasenkov, "Effect of anisotropic scattering of electrons by CF4 on electron transport," *Phys. Lett. Sect. A Gen. At. Solid State Phys.*, vol. 258, no. 2–3, pp. 149–152, 1999, doi: 10.1016/S0375-9601(99)00368-0.

[64] T. Wentink and L. Isaacson, "Radiative lifetimes in the N2Vegard-Kaplan system," *The Journal of Chemical Physics*, vol. 46, no. 2. pp. 822–823, 1967, doi: 10.1063/1.1840756.

[65] A. Lo, G. Cléon, P. Vervisch, and A. Cessou, "Spontaneous Raman scattering: A useful tool for investigating the afterglow of nanosecond scale discharges in air," *Appl. Phys. B Lasers Opt.*, vol. 107, no. 1, pp. 229–242, 2012, doi: 10.1007/s00340-012-4874-3.

[66] A. Montello, Z. Yin, D. Burnette, I. V. Adamovich, and W. R. Lempert, "Picosecond CARS measurements of nitrogen vibrational loading and rotational/translational temperature in

non-equilibrium discharges," *J. Phys. D. Appl. Phys.*, vol. 46, no. 46, 2013, doi: 10.1088/0022-3727/46/46/464002.

[67]   S. Van Alphen, V. Vermeiren, T. Butterworth, D. C. M. Van Den Bekerom, G. J. Van Rooij, and A. Bogaerts, "Power Pulsing to Maximize Vibrational Excitation Efficiency in N2 Microwave Plasma: A Combined Experimental and Computational Study," *J. Phys. Chem. C*, 2019, doi: 10.1021/acs.jpcc.9b06053.

[68]   A. I. Osipov and A. V. Uvarov, "Stability problems in a non-equilibrium gas," *Phys. - Uspekhi*, vol. 39, no. 6, pp. 597–608, 1996.

[69]   F. Esposito, I. Armenise, and M. Capitelli, "N – N 2 state to state vibrational-relaxation and dissociation rates based on quasiclassical calculations," *Chem. Phys.*, vol. 331, pp. 1–8, 2006, doi: 10.1016/j.chemphys.2006.09.035.

[70]   L. G. Piper, "The excitation of N(2P) by N2(A 3Σ u+, v'=0,1)," *J. Chem. Phys.*, vol. 90, no. 12, pp. 7087–7095, 1989, doi: 10.1063/1.456237.

[71]   H. Coitout, G. Cernogora, and L. Magne, "Nitrogen Atoms and Triplet States N2 (B3 Pi g), N2 (C3 Pi u) in Nitrogen Afterglow," *J. Phys. III*, vol. 5, no. 2, pp. 203–217, 1995, doi: 10.1051/jp3:1995120.

[72]   J. C. F. Wang and G. S. Springer, "Vibrational relaxation times in some hydrocarbons in the range 300–900°K," *J. Chem. Phys.*, vol. 59, no. 12, pp. 6556–6562, 1973, doi: 10.1063/1.1680034.

[73]   C. J. S. M. J. S. M. Simpson, T. R. D. R. D. Chandler, and A. C. C. Strawson, "Vibrational relaxation in CO2and CO2-Ar mixtures studied using a shock tube and a laser-schlieren technique," *J. Chem. Phys.*, vol. 51, no. 5, pp. 2214–2219, 1969, doi: 10.1063/1.1672319.

[74]   R. D. Sharma, "Raman scattering by ground-state atomic oxygen," *J. Geophys. Res. Sp. Phys.*, vol. 109, no. A7, pp. 1–6, 2004, doi: 10.1029/2004JA010386.